Draft version April 16, 2012
Preprint typeset using LaTeX style emulateapj v. 03/07/07

IN THE CRUCIBLE: MASSIVE COMPACT GALAXIES WITH HIGH-VELOCITY OUTFLOWS AND EDDINGTON-LIMITED STAR FORMATION

Aleksandar M. Diamond-Stanic[1,2], John Moustakas[1], Christy A. Tremonti[3], Alison L. Coil[1], Ryan C. Hickox[4], Aday Robaina[5], Gregory H. Rudnick[6], & Paul Sell[3]

Draft version April 16, 2012

ABSTRACT

Based on infrared photometry from the Wide-field Infrared Survey Explorer (WISE) and optical morphologies from the Hubble Space Telescope (HST), we present the discovery of compact, obscured star formation in galaxies that exhibit 1000 km s^{-1} outflows. The implied star formation rate (SFR) surface densities approach $\Sigma_{\rm SFR} = 5000$ $M_\odot$ yr^{-1} kpc^{-2}, and we argue that feedback associated with this starburst event is a likely mechanism for launching the high-velocity outflows.

Subject headings: keywords

1. INTRODUCTION

The central regions of elliptical galaxies are thought to form in compact starbursts (e.g., Kormendy et al. 2009; Hopkins et al. 2009). Feedback associated with such starbursts can produce outflows driven by thermal energy from supernova explosions (e.g., Chevalier & Clegg 1985), stellar winds (e.g., Leitherer et al. 1992), and momentum input from both supernova ram pressure and radiation pressure on dust grains (e.g., Murray et al. 2005). It has been argued that such feedback imposes a limit on the maximum star-formation rate surface density ($\Sigma_{\rm SFR}$) for starbursts (e.g., Lehnert & Heckman 1996; Meurer et al. 1997; Murray et al. 2005; Thompson et al. 2005) and the maximum stellar surface density for elliptical galaxies and star clusters (e.g., Hopkins et al. 2010).

Galactic winds are ubiquitous in star-forming galaxies at all redshifts and generally exhibit outflow velocities in the 100–500 km s^{-1} range (e.g., Heckman et al. 2000; Shapley et al. 2003; Martin 2005; Rupke et al. 2005; Weiner et al. 2009; Rubin et al. 2010; Steidel et al. 2010). Thus, the discovery of $|v| > 1000$ km s^{-1} outflows in a sample of massive ($M_* \approx 10^{11}$ $M_\odot$) post-starburst galaxies at $z \sim 0.6$ by Tremonti et al. (2007) suggested that a more energetic source, such as feedback from an accreting supermassive black hole (e.g., Silk & Rees 1998; Di Matteo et al. 2005; Debuhr et al. 2012), could have been responsible for launching the winds.

However, it also plausible that feedback from a compact starburst could expel gas with such large velocities. Indeed, there is evidence for a positive correlation between outflow velocity and starburst luminosity (e.g., Martin 2005; Rupke et al. 2005; Tremonti et al. 2007), albeit with significant scatter. Furthermore, Heckman et al. (2011) recently found outflows with maximum velocities reaching -1500 km s^{-1} in a sample of local starbursts with compact nuclei, and argued that such velocities could be explained by feedback from massive stars.

In this Letter, we present results for a sample of massive galaxies at $z \sim 0.6$ that exhibit $|v| \gtrsim 1000$ km s^{-1} outflows, expanding on the sample from Tremonti et al. (2007). We seek to test whether the energetic outflows in these galaxies could have been driven by feedback from starbursts with very large star-formation rate (SFR) surface densities ($\Sigma_{\rm SFR}$). Our analysis combines galaxy sizes obtained with the Hubble Space Telescope (HST) with star-formation rates and stellar masses estimated from WISE, Spitzer, SDSS, and GALEX photometry.

2. ANALYSIS

2.1. *HST/WFC3 Imaging*

Our sample derives from 29 galaxies targeted for HST/WFC3 imaging in programs 12019 and 12272 (PI: C. Tremonti). Using the F814W filter on the UVIS channel, which has $0.04''$ pixels and FWHM = $0.074''$, we obtained 4×10 min exposures in a single orbit for each galaxy. The dithered images were processed with MultiDrizzle[7] to produce science mosaics with $0.02''$ pixels. For each galaxy, we use GALFIT (Peng et al. 2002, 2010) to model the two-dimensional surface brightness profile with a single Sersic component, using stars in the images to construct the model point-spread function (PSF). The Sersic index (n) and effective radius (r_e) are free parameters in the model. In cases where the best-fit model returns $n > 4$, we also fit an $n = 4$ de Vaucouleurs model (de Vaucouleurs 1948), yielding a larger r_e value (due to the covariance between n and r_e), and we use these these larger effective radii in our analysis.

For this paper, we are most interested in the galaxies with the largest $\Sigma_{\rm SFR}$ values, which also have the smallest effective radii. We show the HST images for three high-$\Sigma_{\rm SFR}$ galaxies in Figure 1. In all three cases, the single-component model GALFIT accounts for $> 85\%$ of the total flux. The residuals show diffuse emission that is consistent with these systems being late-stage galaxy mergers after final coalescence, although we defer a detailed comparison of the observed morphologies with expectations from merger simulations to future work.

For the most compact galaxy (J0905+5759, r_e =

[1] Center for Astrophysics and Space Sciences, University of California, San Diego, La Jolla, CA 92093, USA
[2] Center for Galaxy Evolution Fellow
[3] Department of Astronomy, University of Wisconsin-Madison, Madison, WI 53706, USA
[4] Department of Physics and Astronomy, Dartmouth College, Hanover, NH 03755, USA
[5] Institut de Ciéncies del Cosmos, University of Barcelona, Barcelona, Spain
[6] Department of Physics and Astronomy, University of Kansas, Lawrence, KS 66045, USA

[7] http://stsdas.stsci.edu/multidrizzle/

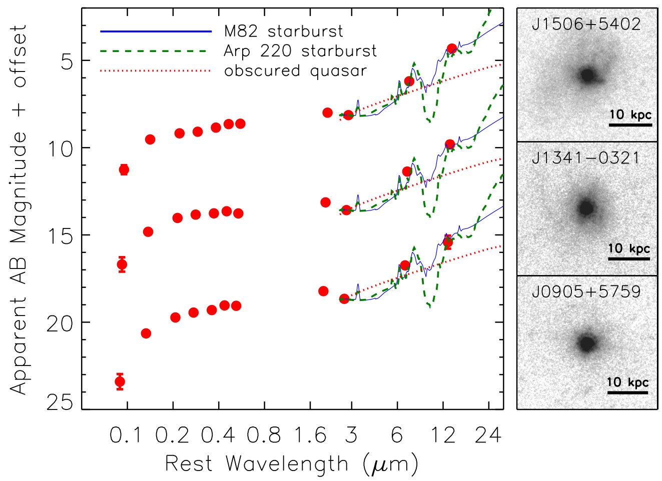

FIG. 1.— Left: Observed UV–IR SEDs ($\lambda_{\rm rest} = 0.1$–15 μm) for three galaxies with large SFR surface densities ($\Sigma_{\rm SFR} >$ 3000 M$_\odot$ yr^{-1} kpc^{-2}). We show stellar population fits to the $\lambda_{\rm rest} = 0.1$–3 μm emission (black solid line) and three templates for dust emission (M82 starburst, Arp 220 starburst, and obscured quasar; Polletta et al. 2007). The starburst templates provide reasonable fits to the $\lambda_{\rm obs} = 12$ and 22 μm WISE photometry, while the quasar template does not. Right: HST/WFC3 F814W images (probing $\lambda_{\rm rest} \approx 5000$ Å) showing that these galaxies are dominated by a compact nucleus.

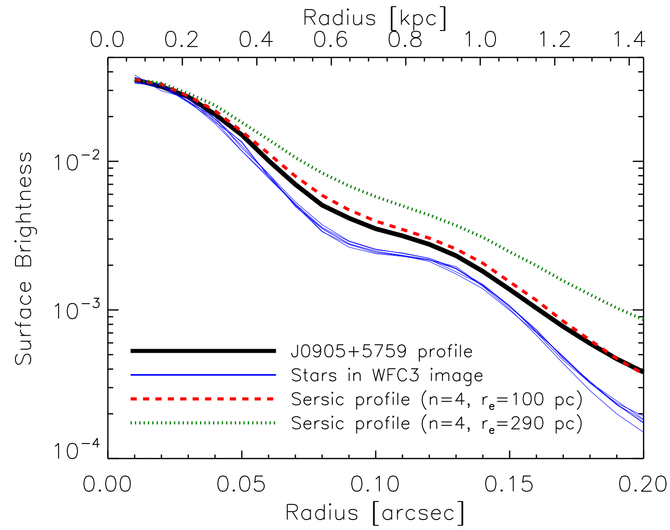

FIG. 2.— One-dimensional surface brightness profile for J0905+5759, which has the smallest effective radius in the sample. The observed profile is shown as the solid black line, and the profiles of six stars in the same image are shown in blue. The best-fit de Vaucouleurs profile with $r_e = 100$ pc is shown as a dashed red line, and for comparison a broader profile with $r_e = 0.04'' = 290$ pc is shown as the dotted green line. This galaxy is quite compact, but is more extended than a point source.

0.013″ or 100 pc), we also show the observed one-dimensional surface brightness profile in the bottom-right panel of Figure 2.1. We compare to the profiles of six stars in the same image, the best-fit de Vaucouleurs model, and a de Vaucoulerus model with a larger effective radius ($r_e = 0.04''$, the native WFC3/UVIS pixel size, which corresponds to a physical scale of 290 pc). This comparison illustrates that this galaxy, while only marginally resolved with an effective radius that is $\sim 20\%$ of the image FWHM, is clearly more extended than a point source.

For such a compact source, there is significant uncertainty in our r_e measurement given uncertainties in the model PSF. To quantify this uncertainty, we used TinyTim to generate a model PSF that is artificially narrower than the stars in the image (convolving the output of tiny2 with a FWHM = 0.04″ Gaussian, whereas the image FWHM is 0.074″) and found that this increased the effective radius in the GALFIT model by a factor of two. We also fit a two-component PSF+Sersic model, but found that the Sersic component dominates the fit, yielding a similar effective radius. Furthermore, the spectrum of the galaxy shows no evidence for an AGN contribution to the I-band continuum (see Figure 3), so there is no clear motivation for including an unresolved, point-source component in the model. We conclude that this galaxy is quite compact and that our r_e estimate of 100 pc, while uncertain, is likely accurate within a factor of two.

2.2. *Photometry, Stellar Masses, and Star-formation rates*

We gathered photometry from the All-Sky Release of the Wide-field Infrared Survey Explorer (WISE, Wright et al. 2010), the Seventh Data Release of the Sloan Digital Sky Survey (SDSS, Abazajian et al. 2009), and General Release 6 from the Galaxy Evolution Explorer (GALEX, Martin et al. 2005). We also obtained 5×30 sec dithered exposures at 3.6 μm and 4.5 μm for all sources with the Infrared Array Camera (Fazio et al. 2004) on the Spitzer Space Telescope (Werner et al. 2004) as part of General Observer program 60145 (PI: C. Tremonti). We used the post–basic calibrated data to perform aperture photometry on all sources, and we also used the APEX[8] point-source extraction software for photometry of sources in crowded fields. All the photometry was corrected for Galactic extinction based on the Schlegel et al. (1998) dust maps. We show spectral energy distributions (SEDs) for the three high-$\Sigma_{\rm SFR}$ galaxies in Figure 1.

We estimate IR-based star-formation rates for the 25/29 galaxies with WISE 12 or 22 μm detections by fitting Chary & Elbaz (2001) templates to their 12 and 22 μm fluxes. For the 14/29 galaxies with 22 μm detections, this yields SFRs that agree with those obtained from the Rujopakarn et al. (2012) method based on 24 μm luminosity (with a scatter of 0.05 dex). We note that several authors have shown that the shape of the IR SED for star-forming galaxies depends on the surface density of star formation (e.g., Rujopakarn et al. 2011; Elbaz et al. 2011), with more compact starbursts having larger total-IR (8–1000 μm) to mid-IR (8–24 μm) ratios. The extreme $\Sigma_{\rm SFR}$ values of our sample imply large total-IR to mid-IR ratios, characteristic of the most luminous galaxies in the local universe (e.g., Chary & Elbaz 2001; Dale & Helou 2002; Rieke et al. 2009). For the 8/29 sources with SFRs in the ULIRG regime ($\mathrm{SFR_{IR}} > 200$ M$_\odot$ yr^{-1}), we would obtain SFRs that are larger by 0.5 dex (compared to the values obtained above) if we used the most luminous local templates.

We also estimate star-formation rates and stellar

[8] http://irsa.ipac.caltech.edu/data/SPITZER/docs/dataanalysistools/tools/m

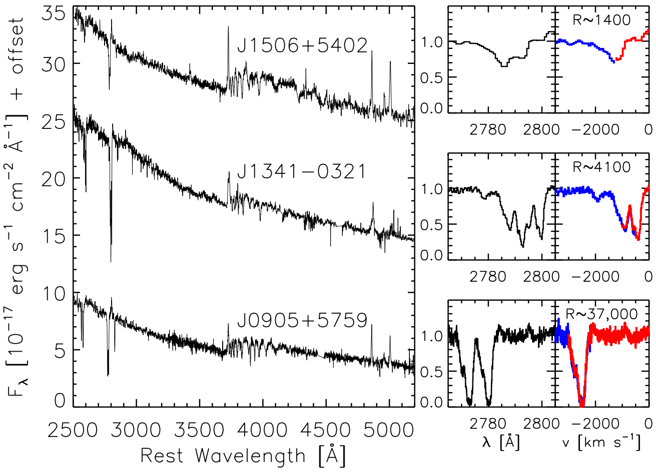

FIG. 3.— Spectra covering $\lambda_{\rm rest}$ = 2500–5200 Å for the three galaxies shown in Figure 1. These spectra are dominated by light from the young stellar population and exhibit [O II] λ3727, Hβ λ4861, and [O III] λ5007 emission lines. The panels on the right zoom on the Mg II $\lambda\lambda$2796, 2803 spectral region in both wavelength and velocity space. The spectrum in the bottom panel has sufficient spectral resolution (FWHM $\approx$ 8 km s^{-1}) to resolve the intrinsic shape of the absorption-line profile, revealing that the gas near the centroid velocity has unity covering factor.

masses based on stellar population fits to the $\lambda_{\rm rest} = 0.1$–3 μm SEDs using the method of Moustakas et al. (2011). For galaxies with SFR$_{\rm IR}$ > 50 M$_\odot$ yr^{-1}, there is agreement between these UV-based SFR estimates and SFR$_{\rm IR}$ with a scatter of 0.32 dex. We find a median extinction of $A_V = 0.4$ mag for an SMC-based dust law.

2.3. *Optical Spectroscopy*

We present low-resolution $R = 1000 - 3000$ spectroscopy from MMT/Blue Channel and SDSS (J1506+5402), Magellan/MagE (J1341-0321), and Keck/LRIS (J0905+5759) in Figure ??. We also highlight the Mg II $\lambda\lambda$2796, 2803 absorption lines, which are used use to measure outflow velocities.

For J0905+5759 we show the Mg II absorption-line profiles from $R \approx 37,000$ spectra obtained with Keck/HIRES. The oscillator strength of Mg II λ2796 is twice that of Mg II λ2803, but the equivalent widths of the two lines and the shapes of the line profiles are quite similar, indicating that both lines are optically thick. The fact that the absorption line profile approaches zero near the velocity centroid $v = -2470$ km s^{-1} indicates that the outflowing gas covers the entire continuum source at these velocities.

3. DISCUSSION

The compact sizes ($r_e \approx 100$ pc) and large star formation rates (SFR $\approx$ 500 M$_\odot$) for the galaxies shown in Figure 1 imply extremely large star-formation rate surface densities ($\Sigma_{\rm SFR} \approx 5000$ M$_\odot$ yr^{-1} kpc^{-2}). To place these galaxies in context, we plot their $\Sigma_{\rm SFR}$ values as a function of stellar mass in Figure 4. We also include measurements of late-stage, gas-rich mergers at $z < 0.3$ from Veilleux et al. (2006), star-forming galaxies at $z < 0.3$ from Overzier et al. (2009), and star-forming galaxies at $z = 1.5$–3.6 from Law et al. (2012).

Points to make:

- Kennicutt (1998), the standard reference for the relationship between SFR and gas surface density, includes Arp 200 with $\Sigma_{\rm SFR} \approx 10^3$ M$_\odot$ yr^{-1} kpc^{-2} and $\Sigma_{H_2} \approx 5 \times 10^{10}$ M$_\odot$ kpc^{-2}.

- The star clusters considered by Meurer et al. (1997) extend into this $\Sigma_{\rm SFR} > 10^3$ M$_\odot$ yr^{-1} kpc^{-2} range.

3.1. *Momentum Flux from Supernovae and Stellar Winds*

Meurer et al. (1997) argued for a limit near 45 M$_\odot$ yr^{-1} kpc^{-2}(somewhat smaller for a Chabrier IMF) based on the surface brightness of starbursts measured using rest-frame UV, Hα, far-IR, and radio continuum emission, such that only 10% of starbursts exceeded this limit. They argued that the momentum flux from supernovae and stellar winds expected at this threshold matches the mean central pressure measured by Heckman et al. (1990) for starburst-driven winds.

There are also relevant arguments about ram pressure driving of high-velocity winds from Heckman et al. (2011).

3.2. *The Eddington Limit from Radiation Pressure on Dust Grains*

In models where gaseous outflows are driven by radiation pressure from massive stars, estimates of the maximum $\Sigma_{\rm SFR}$ where the outward force from radiation exceeds the inward force of gravity are in the $\Sigma_{\rm SFR} \sim 10^3$ M$_\odot$ yr^{-1} kpc^{-2} range (e.g., Thompson et al. 2005; Hopkins et al. 2010).

The relative importance of momentum injection versus thermal heating may vary as a function of galaxy mass (e.g., Hopkins et al. 2012), with thermal heating being less efficient in galaxies with larger gas densities and shorter cooling times. Regarding momentum injection, Sharma & Nath (2011) have argued that radiation pressure becomes more important than ram pressure at large SFRs. Massive star clusters with large gas surface densities are the ideal launching point for galactic-scale outflows driven by radiation pressure (e.g., Murray et al. 2011), and the outflow velocities are expected to scale with escape velocity of the most massive star clusters in a galaxy.

3.3. *Outflows at the Escape Velocity*

The observed $\gtrsim 1000$ km s^{-1} outflow velocities we observe correspond approximately to the escape velocities for compact regions (i.e., massive star clusters) with the sizes and masses that we've measured.

$$v_{esc} = \sqrt{2GM_{cl}/r_{cl}} = 2074\,\mathrm{km\ s^{-1}} \left(\frac{M_{cl}}{10^{11}M_\odot}\right)^{1/2} \left(\frac{r_{cl}}{200\ \mathrm{pc}}\right)^{-1/2} \tag{1}$$

Question of whether other observables are plausible.

- Expected velocity dispersion. Some results have suggested that turbulence becomes large at high surface densities, and therefore the velocity dispersion should be large.

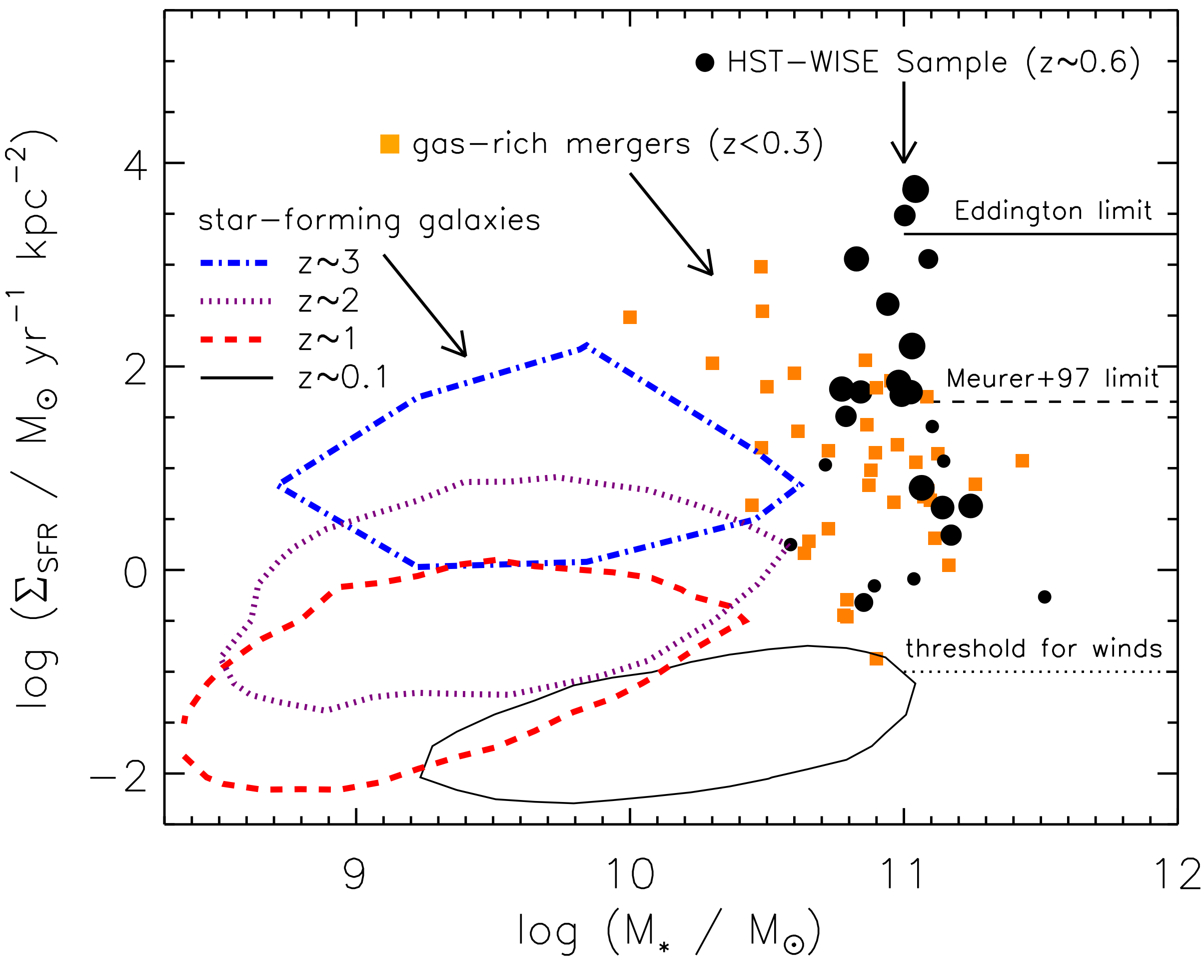

FIG. 4.— SFR surface densities and stellar masses for the HST–WISE sample described in this paper (black circles, with symbol size proportional to outflow velocity), along with samples of gas-rich mergers (orange squares) and star-forming galaxies (shown with 68% contours). We mark the empirical threshold for launching winds (dotted line, $\Sigma_{\rm SFR} = 0.1$ M$_\odot$ yr^{-1} kpc^{-2}; Heckman 2002), the 90th-percentile starburst intensity limit from Meurer et al. (1997) (dashed line, $\Sigma_{\rm SFR} = 45$ M$_\odot$ yr^{-1} kpc^{-2}), and the Eddington limit from radiation pressure on dust grains (solid line, $\Sigma_{\rm SFR} \approx 2000$ M$_\odot$ yr^{-1} kpc^{-2}; Murray et al. 2005; Thompson et al. 2005; Hopkins et al. 2010). Our HST–WISE sample overlaps with the region characterized by gas-rich mergers, and extends to very large SFR surface densities near the Eddington limit. The sample of gas-rich mergers includes ULIRGs (Veilleux et al. 2006), Lyman break analogs with dominant central objects (Overzier et al. 2009), and the local compact starburst Arp 220 (Scoville et al. 1997; Kennicutt 1998; Rodríguez Zaurín et al. 2008). The samples of star-forming galaxies are drawn from Wuyts et al. (2011) at $0.02 < z < 0.2$ (solid black contour), $0.5 < z < 1.5$ (dashed red countour), and $1.5 < z < 2.5$ (dotted purple contour), and from Law et al. (2012) at $2.5 < z < 3.6$ (dash-dotted blue contour).

- The dynamical time for the starburst. If gas is consumed with an efficiency of a few % per dynamical time, how long do we expect the starburst to last?

Other points:

- Is this mechanism viable for the whole sample? We see large outflow velocities in rest of the sample, where the galaxies are more "post" starburst. This fits in a scenario where the genuine post-starbursts are further along in the evolution after the outflow quenches star formation.

- Will these evolve into ellipticals, or do they have enough gas to reform a disk? If they do quench, how difficult would it be to grow in size to match the local size–mass relationship? Could their descendants be the handful of local galaxies that don't lie on the size–mass relationship?

- Is there disagreement between $L_{IR} + L_{UV}$ and Hα SFRs? Heckman et al. (2011) pointed out that this could be a sign of escaping ionizing photons.

3.4. *Limits on Ongoing AGN Activity*

No evidence in spectra for unobscured AGN component. J1506+5402 has X-ray and [Ne V].

3.5. *Placing These Galaxies in Context*

They are rare and thus represent an unusual or short-lived phase.

Connection to models. How such large SFRs given the powerful wind?

Connection to ellipticals. Conceivable that they could grown in size sufficiently by $z = 0$?

We acknowledge useful discussions with and assistance from several people. AMD acknowledges support from the Southern California Center for Galaxy Evolution, a multi-campus research program funded by the University of California Office of Research.

REFERENCES

Abazajian, K. N., Adelman-McCarthy, J. K., Agüeros, M. A., et al. 2009, ApJS, 182, 543
Chary, R., & Elbaz, D. 2001, ApJ, 556, 562
Chevalier, R. A., & Clegg, A. W. 1985, Nature, 317, 44
Crenshaw, D. M., Kraemer, S. B., & George, I. M. 2003, ARA&A, 41, 117
Dale, D. A., & Helou, G. 2002, ApJ, 576, 159
de Vaucouleurs, G. 1948, Annales d'Astrophysique, 11, 247
Debuhr, J., Quataert, E., & Ma, C.-P. 2012, MNRAS, 420, 2221
Di Matteo, T., Springel, V., & Hernquist, L. 2005, Nature, 433, 604
Elbaz, D., Dickinson, M., Hwang, H. S., et al. 2011, A&A, 533, A119
Fazio, G. G., Hora, J. L., Allen, L. E., et al. 2004, ApJS, 154, 10
Granato, G. L., De Zotti, G., Silva, L., Bressan, A., & Danese, L. 2004, ApJ, 600, 580
Heckman, T. M., Armus, L., & Miley, G. K. 1990, ApJS, 74, 833
Heckman, T. M., Lehnert, M. D., Strickland, D. K., & Armus, L. 2000, ApJS, 129, 493
Heckman, T. M. 2002, Extragalactic Gas at Low Redshift, 254, 292
Heckman, T. M., et al. 2011, ApJ, 730, 5
Hopkins, P. F., Cox, T. J., Dutta, S. N., et al. 2009, ApJS, 181, 135
Hopkins, P. F., Murray, N., Quataert, E., & Thompson, T. A. 2010, MNRAS, 401, L19
Hopkins, P. F., Quataert, E., & Murray, N. 2012, MNRAS, arXiv:1110.4638
Kennicutt, R. C., Jr. 1998, ApJ, 498, 541
Kormendy, J., Fisher, D. B., Cornell, M. E., & Bender, R. 2009, ApJS, 182, 216
Law, D. R., Steidel, C. C., Shapley, A. E., et al. 2012, ApJ, 745, 85
Lehnert, M. D., & Heckman, T. M. 1996, ApJ, 472, 546
Leitherer, C., Robert, C., & Drissen, L. 1992, ApJ, 401, 596
Martin, C. L. 2005, ApJ, 621, 227
Martin, D. C., Fanson, J., Schiminovich, D., et al. 2005, ApJ, 619, L1
Meurer, G. R., Heckman, T. M., Lehnert, M. D., Leitherer, C., & Lowenthal, J. 1997, AJ, 114, 54
Moustakas, J., Zaritsky, D., Brown, M., et al. 2011, arXiv:1112.3300
Murray, N., Quataert, E., & Thompson, T. A. 2005, ApJ, 618, 569
Murray, N., Ménard, B., & Thompson, T. A. 2011, ApJ, 735, 66
Overzier, R. A., Heckman, T. M., Tremonti, C., et al. 2009, ApJ, 706, 203
Peng, C. Y., Ho, L. C., Impey, C. D., & Rix, H.-W. 2002, AJ, 124, 266
Peng, C. Y., Ho, L. C., Impey, C. D., & Rix, H.-W. 2010, AJ, 139, 2097
Polletta, M., Tajer, M., Maraschi, L., et al. 2007, ApJ, 663, 81
Rodríguez Zaurín, J., Tadhunter, C. N., & González Delgado, R. M. 2008, MNRAS, 384, 875
Rieke, G. H., Alonso-Herrero, A., Weiner, B. J., et al. 2009, ApJ, 692, 556
Rubin, K. H. R., Weiner, B. J., Koo, D. C., Martin, C. L., Prochaska, J. X., Coil, A. L., & Newman, J. A. 2010, ApJ, 719, 1503
Rujopakarn, W., Rieke, G. H., Eisenstein, D. J., & Juneau, S. 2011, ApJ, 726, 93
Rujopakarn, W., Rieke, G. H., Weiner, B. J., et al. 2011, arXiv:1107.2921
Rupke, D. S., Veilleux, S., & Sanders, D. B. 2005, ApJS, 160, 115
Schlegel, D. J., Finkbeiner, D. P., & Davis, M. 1998, ApJ, 500, 525
Scoville, N. Z., Yun, M. S., & Bryant, P. M. 1997, ApJ, 484, 702
Sharma, M., & Nath, B. B. 2011, arXiv:1112.3447
Shapley, A. E., Steidel, C. C., Pettini, M., & Adelberger, K. L. 2003, ApJ, 588, 65
Shen, S., Mo, H. J., White, S. D. M., et al. 2003, MNRAS, 343, 978
Silk, J., & Rees, M. J. 1998, A&A, 331, L1
Steidel, C. C., Erb, D. K., Shapley, A. E., Pettini, M., Reddy, N., Bogosavljević, M., Rudie, G. C., & Rakic, O. 2010, ApJ, 717, 289
Thompson, T. A., Quataert, E., & Murray, N. 2005, ApJ, 630, 167
Tremonti, C. A., Moustakas, J., & Diamond-Stanic, A. M. 2007, ApJ, 663, L77
Trujillo, I., Conselice, C. J., Bundy, K., et al. 2007, MNRAS, 382, 109
van Dokkum, P. G., et al. 2008, ApJ, 677, L5
Veilleux, S., Kim, D.-C., Peng, C. Y., et al. 2006, ApJ, 643, 707
Weiner, B. J., et al. 2009, ApJ, 692, 187
Werner, M. W., Roellig, T. L., Low, F. J., et al. 2004, ApJS, 154, 1
Wright, E. L., Eisenhardt, P. R. M., Mainzer, A. K., et al. 2010, AJ, 140, 1868
Wuyts, S., Förster Schreiber, N. M., van der Wel, A., et al. 2011, ApJ, 742, 96